

Ca²⁺ Oscillations Mediated by the Synergistic Excitatory Actions of GABA_A and NMDA Receptors in the Neonatal Hippocampus

Xavier Leinekugel, Igor Medina, Ilgam Khalilov,
Yehezkel Ben-Ari, and Roustem Khazipov
INSERM Unité 29
Hôpital de Port-Royal
123, Bd de Port-Royal
75014 Paris
France

Summary

We asked whether GABA_A and NMDA receptors may act in synergy in neonatal hippocampal slices, at a time when GABA exerts a depolarizing action. The GABA_A receptor agonist isoguvacine reduced the voltage-dependent Mg²⁺ block of single NMDA channels recorded in cell-attached configuration from P₂₋₅ CA₃ pyramidal neurons and potentiated the Ca²⁺ influx through NMDA channels. The synaptic response evoked by electrical stimulation of stratum radiatum was mediated by a synergistic interaction between GABA_A and NMDA receptors. Network-driven Giant Depolarizing Potentials, which are a typical feature of the neonatal hippocampal network, provided coactivation of GABA_A and NMDA receptors and were associated with spontaneous and synchronous Ca²⁺ increases in CA₃ pyramidal neurons. Thus, at the early stages of development, GABA is a major excitatory transmitter that acts in synergy with NMDA receptors. This provides in neonatal neurons a hebbian stimulation that may be involved in neuronal plasticity and network formation in the developing hippocampus.

Introduction

The NMDA subtype of glutamate receptors plays an important role in adult and developmental neuronal plasticity via increases in intracellular [Ca²⁺] (Constantine-Paton et al., 1990; Goodman and Shatz, 1993; Malenka and Nicoll, 1993; Fox, 1995; Durand et al., 1996). Since the voltage-dependent Mg²⁺ block of NMDA channels (Mayer et al., 1984; Nowak et al., 1984) operates not only in adult but also in neonatal neurons (LoTurco et al., 1991; Strecker et al., 1994; Crair and Malenka, 1995; Khazipov et al., 1995), their activation during synaptic activity requires external sources of depolarization. In adult neurons, this is largely provided by glutamate acting on AMPA receptors that mediate most of the excitatory drive throughout the mammalian central nervous system. In contrast, GABA, the primary inhibitory transmitter, acting via ionotropic GABA_A receptors (GABA_A R), increases a chloride conductance that usually hyperpolarizes adult neurons, thus preventing the activation of NMDA R (Agmon and O'Dowd, 1992; Kanter et al., 1996). Thus, the induction of NMDA R-dependent forms of long-term potentiation or depression (LTP, LTD) are facilitated by GABA_A R antagonists (Wigstrom and Gustafsson, 1983; Artola and Singer, 1987; Kanter and Haberly, 1993). An opposite situation may prevail at early

stages of development when the activation of GABA_A receptors provides depolarization instead of hyperpolarization (Ben-Ari et al., 1989; 1994; Fiszman et al., 1990; Wu et al., 1992; Hales et al., 1994; Reichling et al., 1994; LoTurco et al., 1995; Serafini et al., 1995; Chen et al., 1996; Rohrbough and Spitzer, 1996). In several types of neonatal neurons, activation of GABA_A R triggers action potentials and activates voltage-dependent Ca²⁺ channels, producing rises of [Ca²⁺]_i (Yuste and Katz, 1991; Hales et al., 1994; Reichling et al., 1994; Leinekugel et al., 1995; LoTurco et al., 1995; Obrietan and van den Pol, 1995; Chen et al., 1996). If GABA is the principal fast-acting excitatory transmitter during early postnatal life in the hippocampus as suggested from earlier studies from this laboratory (Cherubini et al., 1991; Ben-Ari et al., 1994), it may, in contrast to adult neurons, act in synergy with NMDA R, providing the depolarization required to release their voltage-dependent Mg²⁺ block. If so, GABA_A R would play in neonatal neurons the role conferred to AMPA R in more mature neurons. We have now tested this hypothesis in P₂₋₅ neonatal hippocampal slices.

Results

We used cell-attached recordings and noninvasive Ca²⁺ imaging techniques (that do not affect [Cl⁻]) to study the interaction between GABA_A and NMDA receptor-mediated signals in hippocampal slices at postnatal days 2–5 (P₂₋₅).

Isoguvacine Reduces the Mg²⁺ Block of Single NMDA Channels

We examined the effects of the GABA_A-R agonist isoguvacine on single NMDA channel activity recorded in cell-attached configuration from P₂₋₅ pyramidal cells (Figure 1). Action potential-dependent synaptic transmission was blocked by TTX (1 μM in the bath). The activity of NMDA channels in presence of Mg²⁺ was voltage dependent with characteristic flickering at resting membrane potential (estimated to be -82 ± 3 mV from the apparent V_{pipette}) reversal potential of NMDA R-mediated currents, n = 5). The affinity of Mg²⁺ for NMDA channels was estimated using the model of open-channel block (Nowak et al., 1984), as described elsewhere (Khazipov et al., 1995). Bath application of isoguvacine (10 μM) strongly and reversibly reduced the flickering of NMDA channels (Figure 1A), decreasing the Mg²⁺ affinity for NMDA channels (K_{Mg}^{2+} : control: 16.3 ± 5.3 μM; isoguvacine: 118 ± 36 μM; wash: 19.1 ± 4 μM; n = 5; Figure 1B). Because of the configuration used (cell-attached recording), the effect of isoguvacine cannot be due to direct action on the NMDA channels recorded. It was in fact entirely due to depolarization of the cell from -82 ± 3 mV to -59 ± 4 mV (n = 5) as indicated by the positive shift of the apparent V_{pipette} reversal potential of NMDA receptor-mediated currents (Figure 1C).

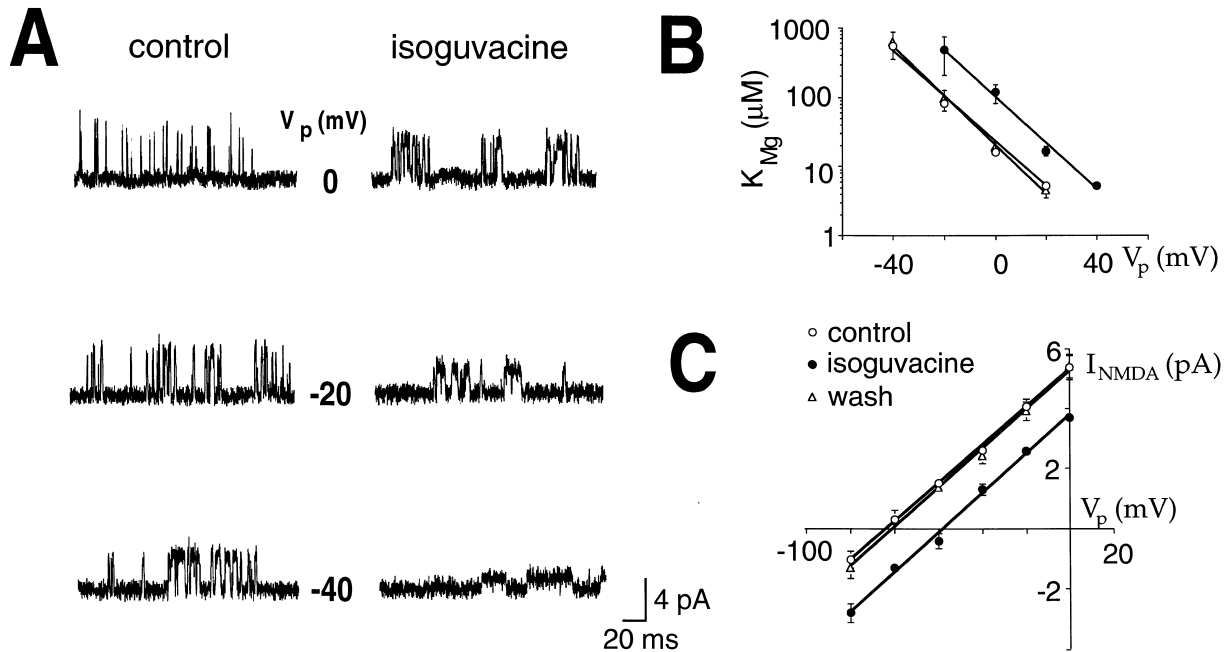


Figure 1. The GABA_A Agonist Isoguvacine Decreases the Voltage-Dependent Mg²⁺ Block of NMDA Channels

Single NMDA channel recordings in the cell-attached configuration from neonatal CA₃ hippocampal pyramidal neurons.

(A) Traces of single NMDA-channels activity recorded at different membrane potentials in control (left) and (right) in presence of isoguvacine (10 μM in the bath). Note the reduction in flickering in presence of isoguvacine.

(B) Plot of Mg²⁺ affinity (mean ± SE; n = 5) at different membrane potentials estimated using the model of open-channel block. Control, open circles; isoguvacine, closed circles; wash, triangles.

(C) Current–voltage relationships of single NMDA channels in control (open circles), in presence (closed circles), and after wash (triangles) of isoguvacine.

Isoguvacine Increases Ca²⁺ Influx through NMDA Channels

If activation of GABA_A receptors facilitates NMDA receptors' activity, it should also increase the Ca²⁺ influx through NMDA channels. In an earlier study, we showed that isoguvacine increases [Ca²⁺]_i via D600 sensitive voltage-dependent Ca²⁺ channels (Leinekugel et al., 1995). We therefore routinely added D600 (50 μM in the bath) to study changes in [Ca²⁺]_i mediated by NMDA R. As shown in Figure 2A, D600 prevented the rise in Ca²⁺ (top lanes) but not the depolarization (lower traces) produced by isoguvacine (100 μM, focal application by pressure ejection) in current-clamp whole-cell recording (internal solution 6: E_{Cl} – around -10 mV). We then used confocal microscopy with the permeant dye Fluo3-AM to measure the Ca²⁺ influx through NMDA channels from nondialyzed P₂₋₅ CA₃ pyramidal cells (Figure 2C). In the presence of D600, neither NMDA (20 μM, bath applied) nor isoguvacine (100 μM, focal application by pressure ejection) alone increased [Ca²⁺]_i (0 ± 3% and +4 ± 3%, respectively; n = 12). In contrast, coapplication of both agonists produced a large [Ca²⁺]_i increase (+158 ± 33%, n = 12). These observations suggest that the depolarization induced by isoguvacine removes the voltage-dependent Mg²⁺ block and thus potentiates Ca²⁺ influx through NMDA R. To exclude possible direct effect of isoguvacine on NMDA channels, we measured NMDA-induced whole-cell currents from freshly dissociated hippocampal neurons (P₃₋₅), in presence of the noncompetitive GABA_A antagonist picrotoxin (10 μM). In these

conditions, isoguvacine did not affect NMDA responses (180 ± 37 pA in control, 178 ± 37 pA in presence of isoguvacine; V_h = -50 mV; n = 5) (data not shown), suggesting that the effects of isoguvacine on NMDA R-mediated Ca²⁺ increase are mediated by the GABAergic depolarization. In keeping with this hypothesis, blocking the isoguvacine-mediated depolarization by voltage clamping the cell at -80 mV during whole-cell recording (Figure 2B, lower lanes) prevented the rise in [Ca²⁺]_i (+2 ± 6%; n = 3) that was observed during coapplication of isoguvacine and NMDA in current-clamp mode (+33 ± 8%; n = 3) (Figure 2B, upper lanes). Therefore, the depolarization produced by GABA_A receptors in conditions that do not affect [Cl⁻]_i reduces the Mg²⁺ block of NMDA channels, thus facilitating NMDA-mediated current and Ca²⁺ influx. We then investigated the interaction between GABA_A and NMDA R-mediated signals in synaptic activity.

Synaptically Activated GABA_A and NMDA Receptors

The neonatal hippocampal network is characterized by the presence of spontaneous and evoked network-driven Giant Depolarizing Potentials (GDPs: Ben-Ari et al., 1989; Gaiarsa et al., 1990). GDPs were described as primarily GABAergic based on their sensitivity to the GABA_A-R antagonist bicuculline and their reversal potential (Ben-Ari et al., 1989). Yet, GDPs are readily blocked by the NMDA-R antagonist APV, suggesting a possible contribution of GABA_A and NMDA R in their

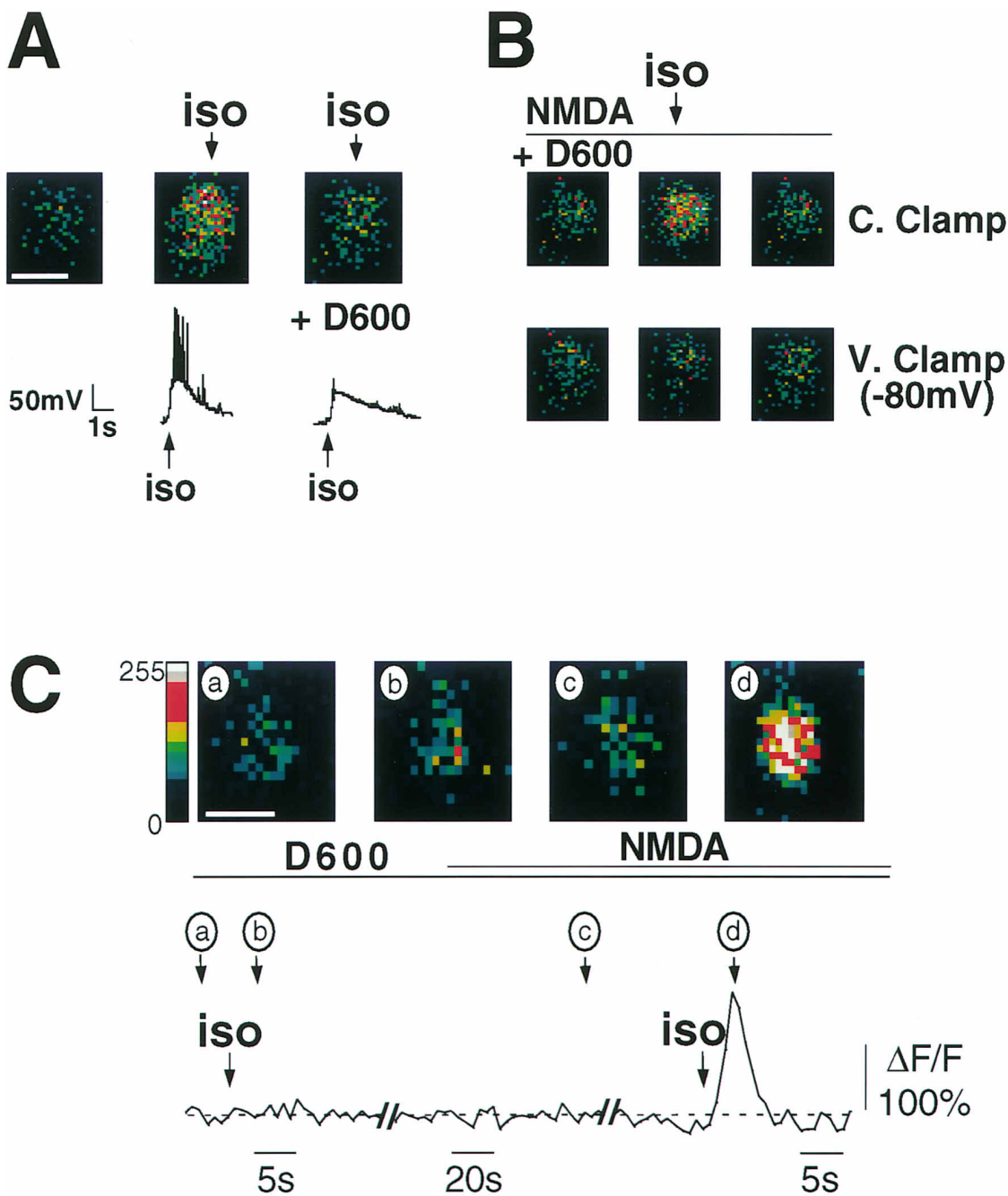


Figure 2. Isoguvacine Potentiates Ca^{2+} Influx through NMDA Receptors Via Depolarization

(A–B) A CA₃ pyramidal cell was loaded with the impermeant dye Fluo-3 through a patch pipette and recorded in whole-cell configuration (internal solution 6: E_{Cl}^- around -10 mV).

(A) Electrophysiological responses (downward traces: current-clamp mode, $V_r = -75$ mV) to pressure application of isoguvacine in control (left trace) and in presence of D600 (50 μM in the bath) (right trace) and associated intracellular $[\text{Ca}^{2+}]_i$ levels (upper lanes: corresponding pseudocolored photomicrographs of the fluorescence; left, control; middle, isoguvacine; and right, isoguvacine in presence of D600). Note that D600 blocked the Ca^{2+} rise but not the depolarization produced by isoguvacine.

(B) Successive (from left to right) pseudocolored photomicrographs of the fluorescence collected in the presence of D600 (50 μM in the bath) and NMDA (20 μM in the bath) before (left), during (middle), and after (right) pressure application of isoguvacine in current clamp ([B] upper lane: $V_r = -75$ mV) and voltage clamp ([B] lower lane: $V_h = -80$ mV) modes. Note that blocking the isoguvacine-mediated depolarization by voltage clamping the cell prevents the Ca^{2+} rise produced by the coapplication of isoguvacine and NMDA.

(C) A P₅ CA₃ pyramidal cell was loaded extracellularly with the Ca^{2+} -sensitive dye Fluo3-AM. The slice was continuously superfused with ACSF containing the voltage-dependent Ca^{2+} channels antagonist D600 (50 μM). The effects of NMDA (20 μM in the bath) and of isoguvacine (100 μM ; 100 ms; focal pressure ejection) on $[\text{Ca}^{2+}]_i$ in the cell presented in the upper lanes (pseudocolored photomicrographs of the fluorescence collected at the corresponding time points, arrows a-d; scale bar, 10 μm) are quantified as changes in $\Delta F/F$ over time (lower traces) from three consecutive acquisition frames (left and right traces, 2 images/s; middle trace, 1 image/4 s).

expression (Corradetti et al., 1988; Ben-Ari et al., 1989). With cell-attached recordings (Figure 3), the electrical stimulation of the s. radiatum evoked with a variable latency (in the range of 20–150 ms) a burst of action potentials (3.9 ± 0.4 a.p.; $n = 13$) that corresponded to GDP when the patch was subsequently broken into whole-cell configuration (not shown). Bath application of CNQX (10 μ M) at a concentration that fully blocks AMPA R in these neurons (McBain and Dingledine, 1992; McLean et al., 1995; I. Khalilov, unpublished data) slightly reduced the response (3.6 ± 0.5 a.p.; $n = 13$) that was abolished by further addition of bicuculline (not shown). Application of APV (50 μ M), in presence of CNQX, significantly reduced the response to 1.4 ± 0.1 a.p. ($n = 13$), which were abolished by further addition of bicuculline (0 a.p.; $n = 13$) (Figure 3). These results suggest that GABA_A and NMDA R may act in synergy to generate GDPs and bursts of action potentials.

To determine whether GABA_A and NMDA R are synaptically coactivated during GDPs in CA₃ pyramidal neurons, we selectively blocked GABA_A R in the recorded neuron by whole-cell dialysis with CsF⁻ + DIDS, MgATP-free pipette solution (solution 5) as described by Nelson et al. (1996) (Figure 4). Synaptic responses were recorded in presence of CNQX (10 μ M). At the beginning of recording, the evoked GDP was largely mediated by Cl⁻ permeable GABA_A R as shown by their negative reversal potential (-54 ± 4 mV; $n = 7$). After 20–30 min of dialysis, we observed that this response reversed around 0 mV (4 ± 2 mV; $n = 7$) and rectified at negative potentials, as expected for NMDA R-mediated currents (Figure 4). These results suggest that GDPs provide coactivation of GABA_A and NMDA R. Similar results ($n = 7$; not shown) could be obtained during longer dialysis (about 1 hr), in absence of DIDS in the pipette (internal solution 4), as recently reported by Khalilov et al. (1996, Soc. Neurosci. abstract). Since GDPs also occur spontaneously (Ben-Ari et al., 1989; Gaïarsa et al., 1990), we suggest that synergistic actions of GABA_A and NMDA R occur during spontaneous synaptic activity in neonatal CA₃ pyramidal cells.

GABA_A and NMDA R-Dependent GDPs Provide Synchronized Neuronal Activity Associated to Ca²⁺ Oscillations

If GDPs provide a coactivation of GABA_A and NMDA receptors, they should be associated with increases in intracellular Ca²⁺. Moreover, since GDPs were synchronously generated in pairs of simultaneously recorded CA₃ pyramidal neurons (cell-attached and whole-cell configurations; $n = 7$ pairs; Figure 5) and associated with a burst of 2–7 action potentials (3.4 ± 0.3 a.p.; $n = 7$; Figures 5A and 5B), these rises in [Ca²⁺] should be synchronous. P₂₋₅ CA₃ pyramidal cells were loaded by focal pressure application of the fluorescent dye Fluo3-AM to monitor spontaneous changes in [Ca²⁺]. As described in earlier studies (Leinekugel et al., 1995), this technique allows loading of several adjacent cells in neonatal slices without modifying the intracellular milieu.

We observed that these cells had spontaneous synchronized [Ca²⁺] increases ($n = 97$ cells from 14 slices) (Figures 6A and 6B). Subsequent whole-cell recordings

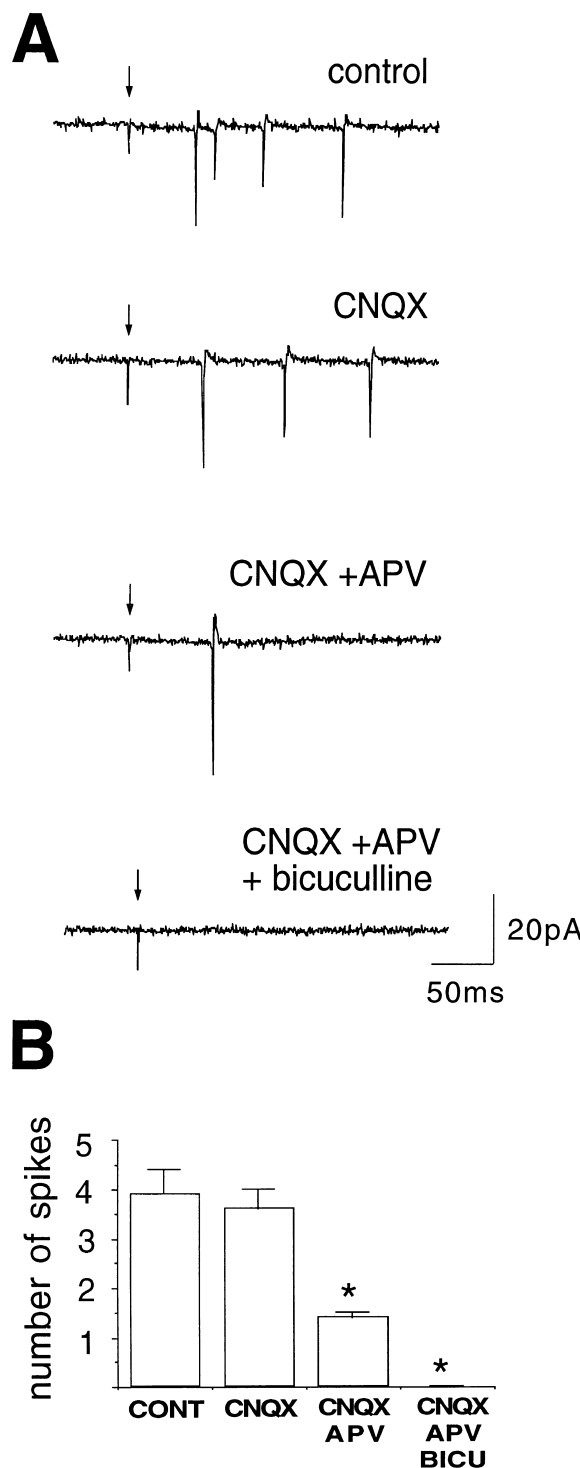


Figure 3. Synaptic Interaction between GABA_A and NMDA Receptors
(A) Synaptic responses of a CA₃ pyramidal neuron from a neonatal (P₅) hippocampal slice were evoked by electrical stimulation of s. radiatum and recorded in the cell-attached configuration. Each large downward deflection corresponds to the firing of an action potential by the recorded cell. Drugs were added to the bath to the following concentrations: CNQX (10 μ M), APV (50 μ M), and bicuculline (10 μ M).

(B) Plot of mean results (mean \pm SE; asterisk, $p < 0.05$) obtained by the same procedures as in (A) in 13 different cells (P₂₋₅).

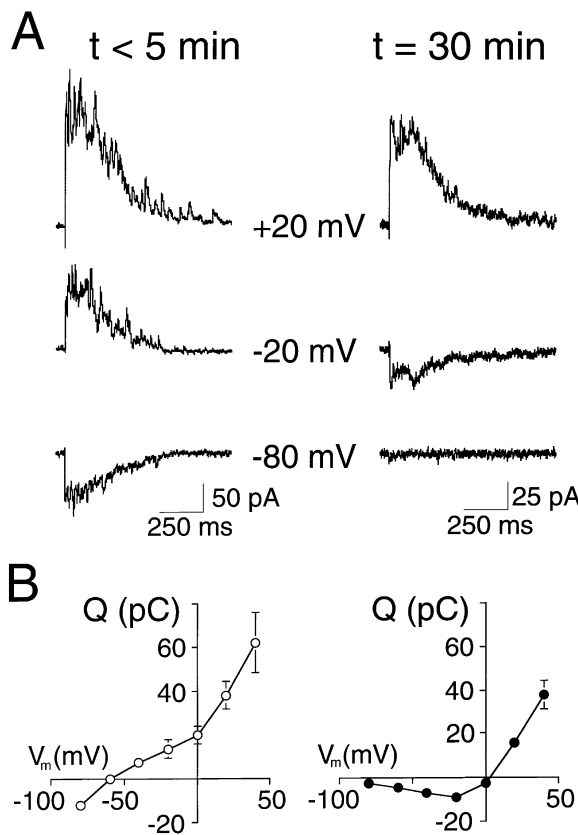


Figure 4. Coactivation of GABA_A and NMDA Receptors during Synaptic Responses

(A) CA₃ pyramidal cells were dialyzed with a pipette solution containing CsF+DIDS (whole-cell recording; internal solution 5). Synaptic responses that correspond to GDPs were evoked by electrical stimulation in the s. radiatum in the presence of the AMPA-R antagonist CNQX (10 μM). Synaptic responses evoked in one neuron at different membrane potentials are presented at the beginning (left) and after 30 min dialysis (right).

(B) The relationship between the current charge of these events and the membrane potential is plotted at the beginning (left) and after (right) dialysis ($n = 7$). Note that during dialysis, the C-V curve changed from nearly linear to strongly rectifying at negative potentials while the reversal potential shifted toward 0 mV, revealing the NMDA component of GDPs.

(with Lucifer Yellow in the pipette solution) of the cells that displayed these Ca^{2+} increases ($n = 17$ cells from 11 experiments) revealed typical morphological (characteristic shape of soma and initial dendrites) and electrophysiological properties (discharge of action potentials and presence of synaptic activity including GDPs) of pyramidal neurons (Figure 6C).

Recording of $[\text{Ca}^{2+}]_i$ transients in groups of CA₃ pyramidal cells simultaneously with whole-cell recording from an additional neuron (pyramidal cells: $n = 17$ experiments; or CA₃ s. radiatum interneurons: $n = 4$ experiments) showed that the $[\text{Ca}^{2+}]_i$ increases were synchronized with the GDPs recorded in that neuron ($\Delta F/F: +51 \pm 4\%$ at the peak; $n = 81$ cells from 14 different slices recorded during 3–20 GDPs), returning to control values about 1–4 s later (Figures 6D–6F). In the vast majority of slices, these GDP-induced Ca^{2+} increases were quite regular, occurring at a rate of 0.05–0.2 s⁻¹.

The coactivation of GABA_A and NMDA R during spontaneous and evoked GDPs should provide a Ca^{2+} influx through NMDA channels. However, exogenous and synaptic activation of GABA_A receptors in P₂₋₅ slices also increases $[\text{Ca}^{2+}]_i$ via VDCC (Leinekugel et al., 1995). To distinguish between these two sources of Ca^{2+} influx, we loaded cells with Fluo3 in the whole-cell configuration and analyzed $[\text{Ca}^{2+}]_i$ changes in the soma either (i) in current-clamp mode that allows the activation of VDCC and NMDA R or (ii) in voltage-clamp mode at depolarized potentials (-30 mV) to allow the activation of NMDA R but not VDCC that rapidly inactivate. During GDPs, large Ca^{2+} increase was observed in current-clamp conditions ($V_h = -75$ mV: $+61 \pm 19\%$, $n = 8$; internal solution 6: E_{Cl}^- around -10 mV) but not in voltage-clamp conditions ($V_h = -30$ mV: $+2 \pm 1\%$; $n = 8$) (Figure 7). Therefore, VDCC but not NMDA R provide Ca^{2+} influx to the soma during GDPs. We suggest that NMDA R that are activated during GDPs might however provide local Ca^{2+} influx at the location of glutamatergic synapses in dendrites (Müller and Connor, 1991; Reger and Tank, 1992; Durand et al., 1996).

Discussion

Our results allow the following conclusions to be drawn. First, during early postnatal life, activation of GABA_A R reduces the voltage-dependent Mg^{2+} block of NMDA channels in CA₃ pyramidal neurons and increases $[\text{Ca}^{2+}]_i$. At these early stages of development, GABA_A and NMDA R act synergistically, GABA_A R playing the role conferred to AMPA R in more adult neurons (Figure 8). Second, the synergistic interaction between GABA_A and NMDA R plays an important role in the generation of network-driven GDPs and associated synchronous Ca^{2+} oscillations that are a major feature of the neonatal hippocampal network.

GABA-NMDA Interaction in the Neonatal Hippocampus

In P₂₋₅ CA₃ pyramidal cells, in conditions that affect neither $[\text{Cl}^-]_i$ nor resting-membrane potential, synaptically activated GABA_A R generate action potentials. These results confirm and extend previous studies reporting depolarizing effects of GABA in neonatal neurons (Ben-Ari et al., 1989; Fiszman et al., 1990; Wu et al., 1992; Hales et al., 1994; Reichling et al., 1994; LoTurco et al., 1995; Serafini et al., 1995; Rohrbough and Spitzer, 1996; Chen et al., 1996). The mechanisms involved in this neonatal GABA_A R-mediated depolarization are not completely understood. The GABA_A receptor-channel complex is primarily Cl^- permeable (Sivilotti and Nistri, 1991; Kaila and Voipio, 1994), and there is a number of evidences for an elevated $[\text{Cl}^-]_i$ in neonatal neurons (Luhmann and Prince, 1991; Zhang et al., 1991; Hara et al., 1992; Serafini et al., 1995; Rohrbough and Spitzer, 1996). Depolarization due to HCO_3^- permeability of GABA_A R (Kaila and Voipio, 1994; Staley et al., 1995) is not necessarily involved in immature neurons since we found that during perfusion with HCO_3^- -free HEPES buffer, isoguvacine still increased Ca^{2+} in neonatal pyramidal cells loaded extracellularly with Fluo3-AM (X. Leinekugel, unpublished data).

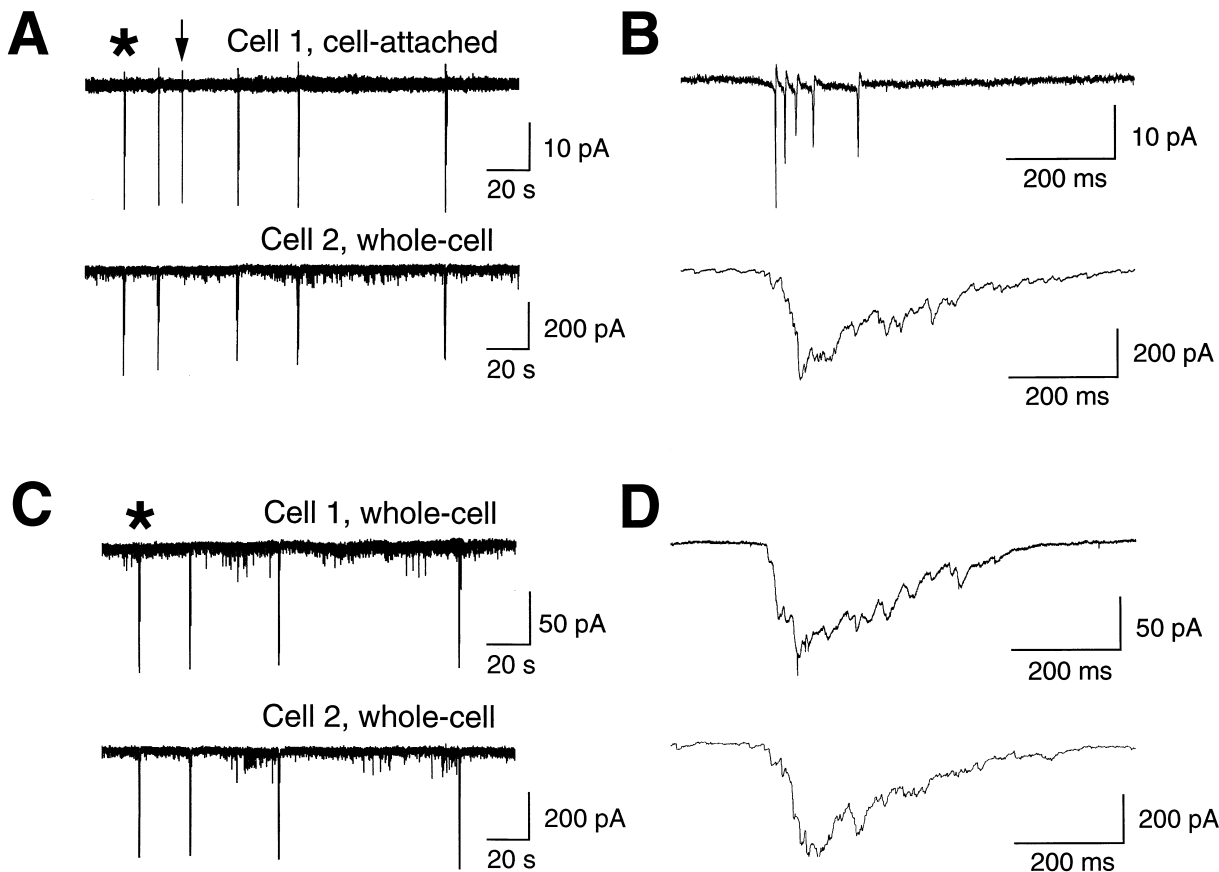


Figure 5. GDPs Are Synchronous in CA₃ Pyramidal Neurons

(A–B) Simultaneous recording of two CA₃ pyramidal cells in the cell-attached (upper trace, cell 1) and whole-cell (lower trace, cell 2) configurations. Note that bursts of action potentials are generated in cell 1 during GDPs in cell 2 (GDP marked by the asterisk in [A] is presented in [B] in expanded time scale) but that spontaneous action potentials can also occur between GDPs ([A]: arrow). (C–D) Entry into the whole-cell mode in cell 1 shows that GDPs are synchronous in both cells (GDP marked by the asterisk in [C] is presented in [D] in expanded time scale). Cell 1: solution 3, V_h = -60 mV; Cell 2: solution 7, V_h = -80 mV.

The fact that blocking AMPA R only slightly affected the synaptic responses evoked by electrical stimulation of s. radiatum is in agreement with other studies suggesting a limited participation of AMPA R in the early synaptic drive to neonatal pyramidal cells (Ben-Ari et al., 1989, 1994; Durand et al., 1996), confirming that GABA is the main fast-acting excitatory transmitter during early postnatal life (Cherubini et al., 1991; Ben-Ari

et al., 1994). Release of the Mg²⁺ block of NMDA channels by the depolarizing effect of GABA_A R during synaptic activity is suggested by the following observations: (i) the depolarization induced by the GABA_A agonist isoguvacine potentiates NMDA R-mediated signals; (ii) synaptically activated GABA_A R provide neuronal excitation; (iii) GABA_A and NMDA R are coactivated during synaptic activity; and (iv) a parallel study conducted

(Figure 6 legend continued)

(C) After Ca²⁺ measurements, the three cells were loaded one by one with Lucifer Yellow using patch pipettes (whole-cell mode; internal solution 3), and spontaneous electrophysiological activities were recorded. Note that morphological (picture) and electrophysiological (recording from cell 2; upper trace: current clamp, V_r = -65 mV; lower trace: voltage clamp, V_h = -60 mV) properties (pyramidal neuronal shape, firing of action potentials, and presence of spontaneous synaptic activity including GDPs) are typical of neonatal hippocampal neuronal cells. Scale bars, 15 μm.

(D–F) In another series of experiments, Ca²⁺-dependent fluorescence changes from a group of CA₃ pyramidal cells loaded with Fluo 3-AM ([D]: pseudocolor fluorescence image from this group of pyramidal cells; CA₃ PYR: CA₃ pyramidal layer; S.R., s. radiatum; scale bar, 15 μm) were monitored during simultaneous whole-cell recording (internal solution 2) of an additional pyramidal cell (not represented). Fluorescence images were collected at the rate of 2/s. Ca²⁺-dependent fluorescence from this group of pyramidal cells was quantified and is presented ([E], upper trace) with the corresponding electrophysiological trace recorded simultaneously from an additional pyramidal cell ([E] downward trace, voltage clamp -60 mV). Note that Ca²⁺ increased synchronously with GDPs.

(F) Mean ± E.S. Ca²⁺-dependent fluorescence responses (upper traces) from three visually identified pyramidal cells from the group presented in (D) (cells 1–3 delimited by white lines) recorded during 20 GDPs (mean trace: downward trace).

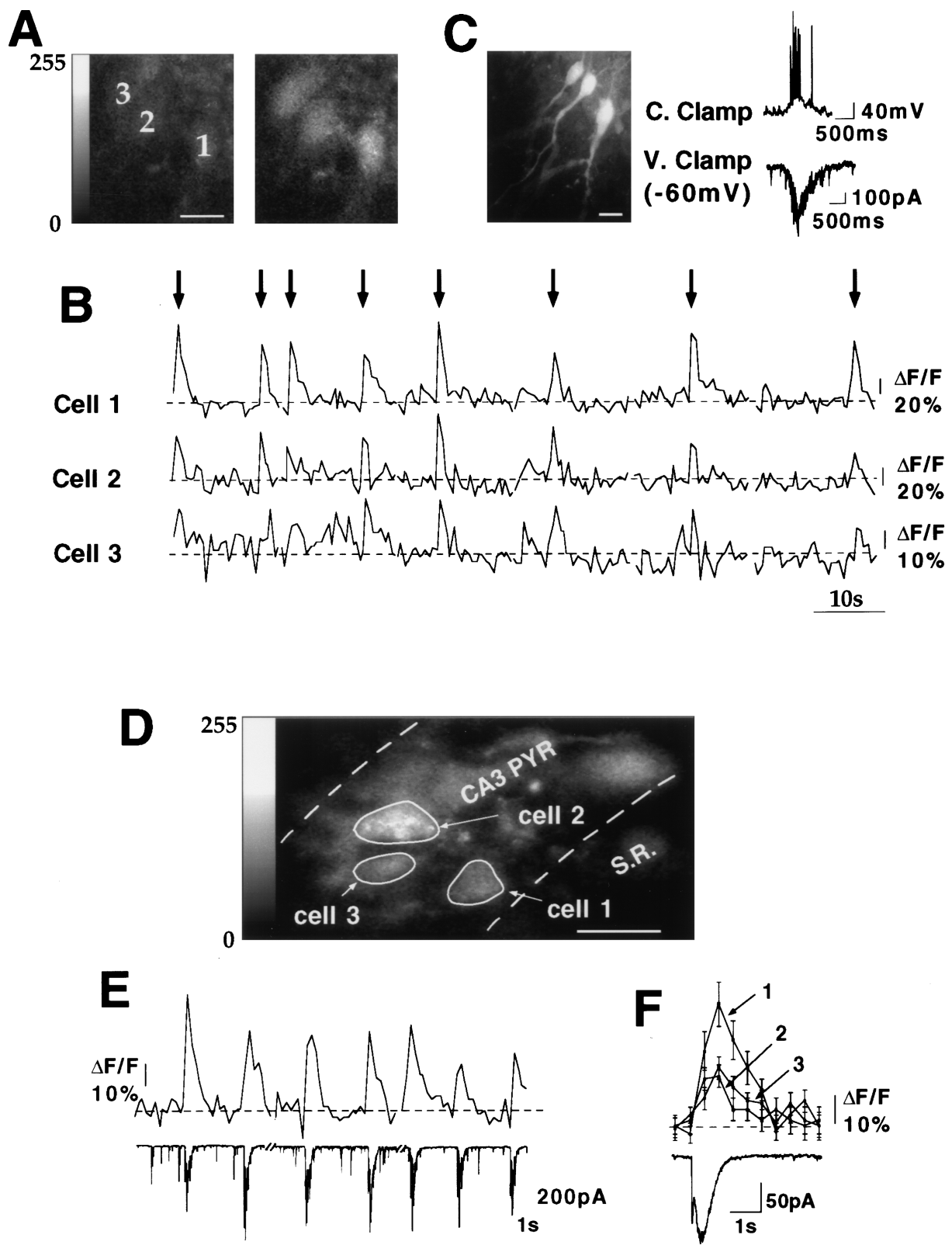


Figure 6. Synchronous Spontaneous Ca^{2+} Oscillations in CA₃ Pyramidal Neurons

(A–C) Three CA₃ pyramidal cells were visually selected and loaded with Fluo 3-AM.

(A) Ca^{2+} -dependent fluorescence images of these three cells (upper lanes: left, resting level; right, peak of Ca^{2+} transient) were acquired at the rate of 2/s, and quantitation is presented in (B). Note that Ca^{2+} transients are synchronous in the three cells.

(Figure 6 legend continued on previous page)

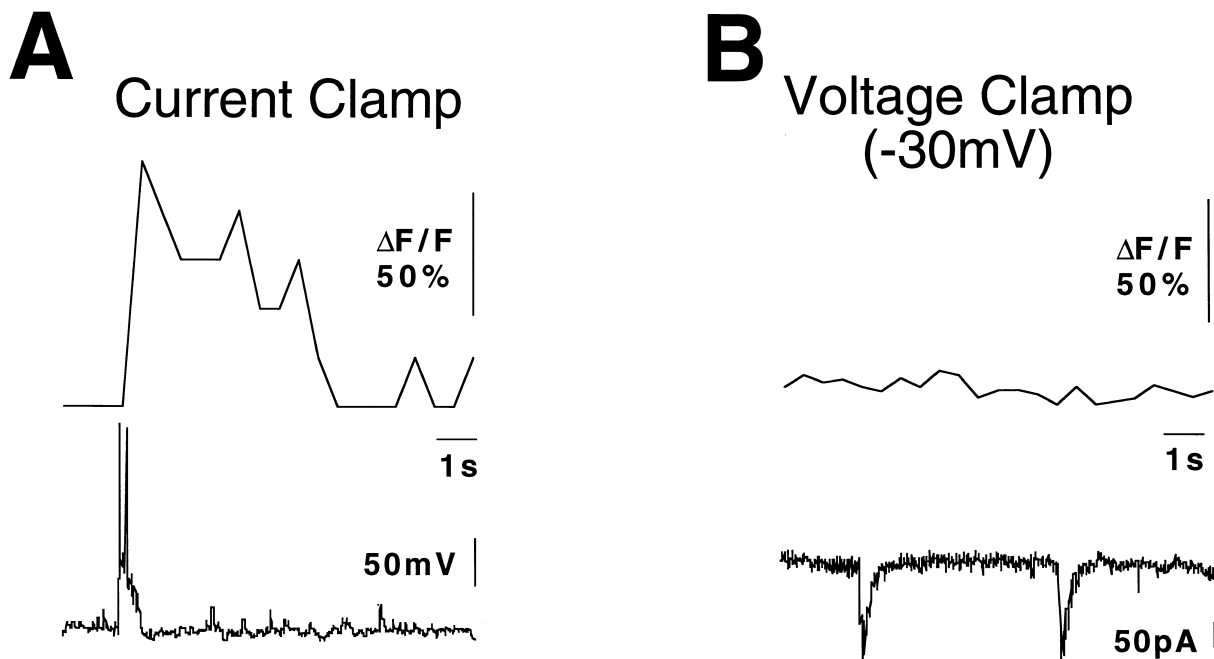


Figure 7. Ca^{2+} Influx Via Voltage-Dependent Ca^{2+} Channels in the Soma during GDPs

Ca^{2+} -dependent fluorescence was monitored during whole-cell recording of GDPs from a pyramidal cell loaded with Fluo-3 through the patch pipette (internal solution 6: E_{Cl}^- about -10 mV). Fluorescence images of the soma were acquired at the rate of 2/s, and quantitation is presented (upper traces) with the simultaneous electrophysiological recordings (lower traces).

(A) In current-clamp mode, GDP produced a depolarization of the cell and an increase in $[\text{Ca}^{2+}]_i$.

(B) In voltage-clamp mode at a potential ($V_h = -30$ mV) that allows NMDA receptors activation but prevents activation of voltage-dependent Ca^{2+} channels, occurrence of GDPs is not accompanied by a rise in Ca^{2+} . These results suggest that there is no detectable Ca^{2+} influx through NMDA channels in the soma during GDPs.

in our laboratory indicated that synergistic actions of synaptically activated GABA_A and NMDA R induced LTD of GABA_A R-mediated synaptic transmission in P_{2-5} CA_3 pyramidal cells. This LTD that is induced by a tetanic stimulation of s. radiatum requires activation of GABA_A and NMDA R and a rise in postsynaptic Ca^{2+} (McLean et al., 1996). Figure 8 schematically depicts the differences between adult and neonatal GABAergic and glutamatergic signals.

The presently described coactivation of GABA_A and NMDA R in CA_3 pyramidal cells during GDPs is in agreement with previously reported sensitivity of GDPs to GABA_A and NMDA-R antagonists (Ben-Ari et al., 1989). However, they are in contradiction with previous results indicating that GDPs were entirely mediated by GABA_A R in CA_3 pyramidal cells (Ben-Ari et al., 1989). This discrepancy might be explained by the differences in experimental approaches. According to Staley and Mody (1992), the increase in conductance that results from activation of GABA_A R largely shunts glutamatergic currents, especially during current-clamp recordings. The earlier experiments of Ben-Ari et al. (1989) showed, in addition to the sensitivity of GDPs to bicuculline, that the voltage changes produced by isoguvacine and by GDPs recorded in current-clamp mode had similar reversal potentials. The large increase in conductance produced by the GABAergic component of GDPs may thus have masked an NMDA component in these conditions, due to shunting mechanisms. Our results are

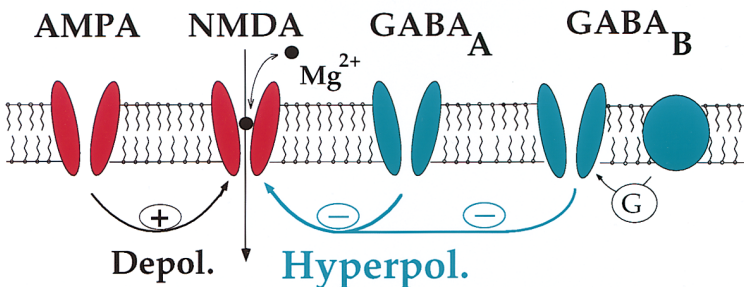
based on a different technical approach that consists of intracellular blockade of GABA_A R, therefore eliminating the GABAergic component of GDPs and associated increase in conductance.

We therefore suggest that the GABA_A R-mediated depolarization, relayed by the subsequent activation of voltage-dependent Na^+ and Ca^{2+} channels, propagates to glutamatergic synapses in dendrites and facilitates expression of NMDA responses during synaptic activity, presumably resulting in local Ca^{2+} influx through NMDA R. GABA also controls intracellular $[\text{Ca}^{2+}]_i$ levels via VDCC that, as in adult neurons, provide the most substantial part of the Ca^{2+} increase during excitatory synaptic transmission (Miyakawa et al., 1992).

Implication for NMDA R-Mediated Signals in the Neonatal Brain

Preferential participation of NMDA R in neonatal synaptic transmission has been reported in several brain structures (Tsumoto et al., 1987; Ben-Ari et al., 1989, 1994; Fox et al., 1989; Constantine-Paton et al., 1990; Gaiarsa et al., 1990; Yuste and Katz, 1991; Agmon and O'Dowd, 1992; Crair and Malenka, 1995). Electrophysiological investigation in visual and somatosensory cortex and in the hippocampus of the NMDA-AMPA ratio suggested a development of glutamatergic transmission from predominantly NMDA-R mediated during the early stages of development to predominantly AMPA-R mediated subsequently (Ben-Ari et al., 1994; Crair and Malenka,

ADULT



NEONATE

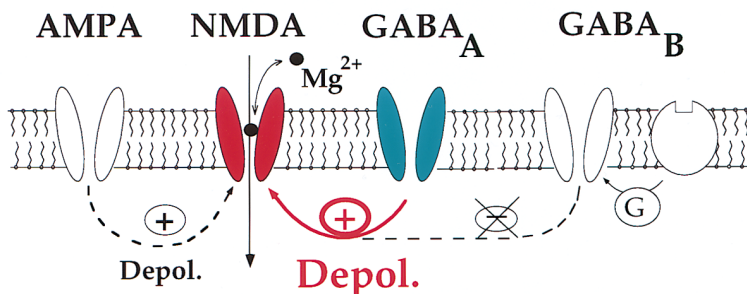


Figure 8. Major Developmental Changes in the GABA–Glutamate Interactions

In adult neurons, activation of AMPA receptors provides the excitatory drive necessary to remove the voltage-dependent Mg^{2+} block of NMDA channels while GABA, acting on GABA_A and GABA_B receptors, provides hyperpolarization and inhibits NMDA receptor-mediated signals. In neonatal neurons, postsynaptic GABA_B receptors are not functional, and depolarizing effects of GABA, acting via GABA_A receptors, reduce the voltage-dependent Mg^{2+} block of NMDA channels, providing synergy between GABA and glutamate. AMPA receptor-mediated transmission is weak in the early periods of development.

1995; Durand et al., 1996). Several factors are implicated in the preferential participation of NMDA R in neonatal neurons: delayed development of G protein-mediated (including GABA_B) postsynaptic inhibition (Fukuda et al., 1993; Gaïarsa et al., 1995), higher density of NMDA R in humans and rats (Tremblay et al., 1988; Represa et al., 1989), and slower kinetics of NMDA responses (Hestrin, 1992; Carmignoto and Vicini, 1992; Fox, 1995; Khazipov et al., 1995) that may be due to different expression of NMDA-R subunits in neonatal neurons (Pollard et al., 1993; Monyer et al., 1994). However, the voltage-dependent Mg^{2+} block of NMDA channels seems to be efficient at all stages of development (LoTurco et al., 1991; Strecker et al., 1994; Crair and Malenka, 1995; Khazipov et al., 1995; Durand et al., 1996), suggesting that a powerful excitatory drive is required to activate NMDA receptors. We suggest that GABA exerts this role in the neonates. This may, in addition to the above-mentioned mechanisms, explain the large participation of NMDA R in the neonatal synaptic drive. The depolarizing effects of GABA have been reported during the early periods of development in all brain structures studied thus far (Ben-Ari et al., 1989; Yuste and Katz, 1991; Gaïarsa et al., 1995; LoTurco et al., 1995; Obrietan and van den Pol, 1995; Serafini et al., 1995; Rohrbough and Spitzer,

1996), and a shift from de- to hyperpolarizing effects of GABA is also observed in neurons in cultures (Wang et al., 1994; Obrietan and van den Pol, 1995; Chen et al. 1996). Therefore, the excitatory effects of GABA as well as the GABA–NMDA synergy may represent a fundamental property of developing networks.

Implications for Developmental Plasticity

GABA and glutamate have multiple morphogenic and trophic effects in developing neurons (Redburn and Schousboe, 1987; Spoerri, 1988; Belhage et al., 1988; Scherer and Udin, 1989; Constantine-Paton et al., 1990; Goodman and Shatz, 1993; Barbin et al., 1993; Rakic and Komuro, 1995; Behar et al., 1996) via changes in the intracellular Ca^{2+} , control of DNA synthesis, and growth factors expression (Lipton and Kater, 1989; Launder, 1993; LoTurco et al., 1995; Marty et al., 1996). The present study describes how the changes in Ca^{2+} homeostasis and possibly related trophic effects of these neurotransmitters occur during physiological patterns of activity in the neonatal hippocampus.

Synchronous neuronal activity represents a fundamental property of the developing neuronal networks (Ben-Ari et al., 1989; Gaïarsa et al., 1990; O'Donovan et al., 1992; Kandler and Katz, 1995; Gu and Spitzer, 1995;

Yuste et al., 1995; Feller et al., 1996), but the mechanisms of synchronization differ. While in the neocortex it is generated by gap junctions (Kandler and Katz, 1995; Yuste et al., 1995), synchronization of neuronal activity clearly implies synaptic mechanisms in retina, via cholinergic transmission (Katz, 1993; Wong et al., 1993; Feller et al., 1996) and in the hippocampus, via the excitatory actions of GABA_A and glutamate receptors (Corradetti et al., 1988; Ben-Ari et al., 1989; Gaïarsa et al., 1990; Hanse et al., Soc. Neurosci. abstract, 1996). We observed that GDPs can also be recorded from interneurons and that they are synchronous with GDPs in pyramidal cells, indicating that GDPs result from the synchronous discharge of pyramidal cells and GABAergic interneurons (Khazipov et al., 1997). The neonatal hippocampal network is organized in recurrent excitatory loops, pyramidal cells and interneurons being excited by the depolarizing effects of GABA and glutamate (Leinekugel et al., 1995), which provide synchronous neuronal discharges (GDPs) largely mediated by GABA_A receptors. These synchronous activities may be implicated in the control of neuronal growth and formation of the neuronal networks via changes in Ca²⁺ homeostasis (Constantine-Paton et al., 1990; Goodman and Shatz, 1993). Although the consequences of the Ca²⁺ influx during GDPs via voltage-gated Ca²⁺ channels and NMDA channels are presently unknown, activation of voltage-gated Ca²⁺ channels promotes differentiation of neurons in several preparations (Desarmenien and Spitzer, 1991; Gu and Spitzer, 1995; LoTurco et al., 1995; Rusanescu et al., 1995). Moreover, localized Ca²⁺ influx through NMDA receptors can provide a hebbian modulation of developing synapses (Komatsu and Iwakiri, 1993; Fox, 1995; Crair and Malenka, 1995; Kirkwood et al., 1995; Durand et al., 1996; McLean et al., 1996) and may be involved in activity-dependent synaptogenesis and network formation.

Experimental Procedures

Slice Preparation

Slices were prepared as described previously (Ben-Ari et al., 1989) from 2- to 5-day-old male Wistar rat pups. In brief, after sacrificing the rat by decapitation, the brain was rapidly removed and placed in oxygenated, ice-cooled artificial cerebrospinal fluid (ACSF); hippocampal transverse slices (thickness 400–500 μm) were cut with either a McIlwain tissue chopper or a vibratome (FTB Vibracut) and kept in oxygenated (95% O₂ and 5% CO₂) ACSF (in mM: 126 NaCl; 3.5 KCl; 2 CaCl₂; 1.3 MgCl₂; 25 NaHCO₃; 1.2 NaH₂PO₄; and 11 glucose, pH 7.3) at room temperature at least 1 hr before use. Individual slices were then transferred to the recording chamber where they were fully submerged and superfused with oxygenated ACSF at 30–32°C at a rate of 2–3 ml/min.

Isolated Neurons Preparation

Neurons were freshly isolated from P_{2–5} hippocampal slices as described (Medina et al., 1994). In brief, slices were incubated at 30°C for 25–30 min in an O₂ atmosphere, in a solution containing (in mM): 115 NaCl, 10 KCl, 1.2 NaH₂PO₄, 10 MgCl₂, 26 NaHCO₃, and 10 glucose, pH 7.4 (solution A), + 1.5 mg/ml protease XXIII. Slices were then washed with solution A for 15 min. The concentration of CaCl₂ was slowly increased up to 1 mM. For dissociation of cells, slices were again transferred to solution A without CaCl₂, and the CA₃ region was dissected and gently agitated by sharp glass needles to release individual cells. Cells were placed in the recording chamber and solution A was replaced slowly (over 10 min) by a solution of the following composition (in mM): 150 NaCl, 1 KCl, 2 CaCl₂, 1

MgCl₂, 10 HEPES, 10 glucose, and 0.01 glycine, pH 7.4. The best results were obtained when slices were allowed to recover for 2–5 hr after protease treatment. For whole-cell recordings, internal solution (pH 7.3; osmolarity 300 mmol/kg) of the following composition was used (in mM): 80 CsCl, 80 Cs-Gluconate, 0.06 CaCl₂, 1.1 BAPTA-Cs₄, 10 HEPES, and 2 MgATP, pH 7.2.

Electrophysiological Recordings

Recordings were performed using the patch-clamp technique in the cell-attached and whole-cell configurations. Microelectrodes had a resistance of 7–10 M Ω . Internal solutions (pH 7.3; osmolarity 270–280 mmol/kg measured by a Knauer osmometer, Berlin) of the following composition were used (in mM): for recordings of single NMDA channels in cell-attached configuration, 1) ACSF with 0.05 Mg²⁺, 1 EGTA, 0.01 NMDA, and 0.01 glycine; for whole-cell recordings in slice: 2) 140 CsCl, 1 CaCl₂, 10 EGTA, and 10 HEPES; or 3) 100 KCl, 10 NaCl, 0.25 CaCl₂, 5 EGTA, 10 HEPES, 10 Glucose, 2 MgATP, and 0.2 GTP; or 4) 140 CsF, 1 CaCl₂, 10 EGTA, and 10 HEPES; or 5) solution 4 + 0.5–1 4,4'-diisothiocyanostilbene-2,2'-disulfonic acid (DIDS); for Ca²⁺-imaging whole-cell recordings: 6) solution 3 + 0.01 Fluo3; for recordings of spikes in cell-attached configuration: 7) 135 K gluconate, 2 MgCl₂, 0.1 CaCl₂, 1 EGTA, 2 Na² ATP, and 10 HEPES. Occasionally, Lucifer Yellow (0.1–1%) was added to solution 3 for morphological monitoring. To isolate the glutamate receptor-mediated component of the evoked synaptic response, the cells were dialyzed, as suggested by Nelson et al. (1996), with internal solution that contained CsF, DIDS, and that did not contain MgATP (solution 5). In some experiments, internal dialysis was performed in absence of DIDS (solution 4). As described elsewhere (Khalilov et al., Soc. Neurosci. abstract, 1996), this procedure completely suppresses exogenous and synaptic GABA_A receptor-mediated responses in the cell under investigation, with only moderate effects on the exogenous and synaptic AMPA and NMDA receptor-mediated responses (10%–30% reduction of NMDA responses). Slices were stimulated by a bipolar tungsten electrode (30–80 V; 10–30 μs ; 0.02–0.05 Hz) placed in the s. radiatum of the CA₃ region of the hippocampus.

Data Analysis

Synaptic-evoked responses were recorded using an Axopatch 200 (Axon Instrument, USA) amplifier, stored into the memory of an 80486 personal computer using TL1 DMA Labmaster A/D converter (USA) and then analyzed using Acquis Software (Gérard Sadoc, France). Axotape and SE04 (USA) programs were used for the acquisition and analysis of spontaneous events. Single-channel currents were recorded at 5 kHz on a tape recorder DTR 1201 (Bio-Logic, France) and then digitized at a sampling frequency of 10 kHz for analysis (p-CLAMP programs, Axon Instruments, USA). Mg²⁺ block of NMDA channels was estimated using the model of open-channel block (Nowak et al., 1984), as described elsewhere (Khazipov et al., 1995). Group measurements were expressed as means \pm SEM. Statistical significance of differences between means was assessed with the Student's *t*-test, with the aid of statistical software StatView SE+ Graphics. The level of significance was set at $p < 0.05$.

Fluorescence Measurements

Fluorescence measurements were performed as described (Leinekugel et al., 1995) on neurons loaded with the Ca²⁺-sensitive dye Fluo-3 either in the impermeant form (whole-cell configuration, internal solution 6) or in the esterified form (Fluo-3 AM: 3.3 μM , applied focally from a micropipette during 5–30 min by 0.3–1 s, 0.2 Hz pressure pulses), using a confocal laser scanning microscope (MRC BIORAD 600) equipped with argon-krypton laser and photomultiplier. Excitation was delivered at 488 nm, and emission intensity was measured at wavelength >500 nm. Images were acquired every 0.5–4 s using the program SOM (BIORAD, USA) and analyzed off-line with the program Fluo (IMSTAR, France). All results were expressed as $\Delta F/F_0$, with F = fluorescence from the defined portion of the image corresponding to the cell(s) under investigation and F₀ = mean baseline fluorescence in the selected area(s) from at least five consecutive images. Because Fluo-3 is a single-wavelength chromophore, and fluorescence is a function of the concentration of Ca²⁺ and dye (Kao et al., 1989), we have used this dye only for

approximate estimation of $[\text{Ca}^{2+}]$, and included for analysis only experiments in which the fluorescence level recovered to control value after cell excitation. As described earlier (Leinekugel et al., 1995), individual neurons were selected using the optics of an axio-scope Karl Zeiss microscope (water immersion objective $\times 40$) that allows recognition of neurons in slices. The neurons were then approached with the Fluo3-AM containing pipette for loading. The use of a calibrated map to correlate fluorescence spots and the visual optical field verified that the fluorescence signals monitored originated from the selected neurons.

Solutions and Drugs

Fluo 3-AM and DIDS were first dissolved in DMSO ($<0.1\%$ final) and just before use in either standard ACSF (Fluo 3-AM) or internal pipette solution (DIDS). NMDA and isoguvacine were dissolved in ACSF and applied by bath. In some experiments, isoguvacine was applied locally by pressure ejection from a micropipette using a Picospritzer II (General Valve, USA). Drugs used were purchased from Sigma (NMDA, tetrodotoxin, D-600, DIDS, and protease XXIII), Tocris Neuramin (isoguvacine, bicuculline, CNQX [6-Cyano-7-nitroquinoxaline-2,3 dione], and glycine), APV ([d-2-Amino-5-phospho-pentanoate]) and Molecular Probes (Fluo3 and Fluo3-AM).

Acknowledgments

We thank Drs. R. Miles, K. Krnjevic, J. L. Gaiarsa, S. Shorte, G. Holmes, and H. A. McLean for useful discussions and critical reading of the manuscript; Dr. A. Bakhrayev for the help in single channels analysis; and B. Martin and S. Weiler for technical assistance in Ca^{2+} images processing. This work was supported by grants from INSERM, Ministère de la Recherche et de l'Espace, Société de Secours des Amis des Sciences, and Association Nationale de Recherche sur le SIDA (AIDS).

References

- Agmon, A., and O'Dowd, D.K. (1992). NMDA receptor-mediated currents are prominent in the thalamocortical synaptic response before maturation of inhibition. *J. Neurophysiol.* 68, 345–349.
- Artola, A., and Singer (1987). Long-term potentiation and NMDA receptors in rat visual cortex. *Nature* 330, 649–652.
- Barbin, G., Pollard, H., Gaiarsa, J.L., and Ben-Ari, Y. (1993). Involvement of GABA_A receptors in the outgrowth of cultured hippocampal neurons. *Neurosci. Lett.* 152, 150–154.
- Behar, T.B., Li, Y.-X., Tran, H.T., Ma, W., Dunlap, V., Scott, C., and Barker, J.L. (1996). GABA stimulates chemotaxis and chemokinesis of embryonic cortical neurons via calcium-dependent mechanisms. *J. Neurosci.* 16, 1808–1818.
- Belhage, B., Hansen, G.H., Schousboe, A., and Meier, E. (1988). GABA agonist promoted formation of low affinity GABA receptors on cerebellar granule cells is restricted to early development. *Int. J. Dev. Neurosci.* 6, 125–128.
- Ben-Ari, Y., Cherubini, E., Corradetti, R., and Gaiarsa, J.L. (1989). Giant synaptic potentials in immature rat CA3 hippocampal neurons. *J. Physiol. (Lond.)* 416, 303–325.
- Ben-Ari, Y., Tsseeb, V., Ragozzino, D., Khazipov, R., and Gaiarsa, J.L. (1994). γ -Aminobutyric acid (GABA): a fast excitatory transmitter which may regulate the development of hippocampal neurones in early postnatal life. *Prog. Brain Res.* 102, 261–273.
- Carmignoto, G., and Vicini, S. (1992). Activity-dependent decrease in NMDA receptor responses during development of the visual cortex. *Science* 258, 1007–1011.
- Chen, G., Trombley, P., and van den Pol, A.N. (1996). Excitatory actions of GABA in developing rat hypothalamic neurones. *J. Physiol. (Lond.)* 494, 451–464.
- Cherubini, E., Gaiarsa, J.L., and Ben-Ari, Y. (1991). GABA: an excitatory transmitter in early postnatal life. *Trends Neurosci.* 14, 515–519.
- Constantine-Paton, M., Cline, H.T., and Debski, E. (1990). Patterned activity, synaptic convergence, and the NMDA receptor in developing visual pathways. *Annu. Rev. Neurosci.* 13, 129–154.
- Corradetti, R., Gaiarsa, J.L., and Ben-Ari, Y. (1988). D-Aminophenoxyvaleric acid-sensitive spontaneous giant EPSPs in immature rat hippocampal neurones. *Eur. J. Pharmacol.* 154, 221–222.
- Craig, M.C., and Malenka, R.C. (1995). A critical period for long-term potentiation at thalamocortical synapses. *Nature* 375, 325–328.
- Desarmenien, M.G., and Spitzer, N.C. (1991). Role of calcium and protein kinase C in development of the delayed rectifier potassium current in *Xenopus* spinal neurons. *Neuron* 7, 797–805.
- Durand, G.M., Kovalchuk, Y., and Konnerth, A. (1996). Long-term potentiation and functional synapse induction in developing hippocampus. *Nature* 381, 71–75.
- Feller, M.B., Wellis, D.P., Stellwagen, D., Werblin, F.S., and Shatz, C.J. (1996). Requirement for cholinergic synaptic transmission in the propagation of spontaneous retinal waves. *Science* 272, 1182–1187.
- Fiszman, M.L., Novotny, E.A., Lange, G.D., and Barker, J.L. (1990). Embryonic and early postnatal hippocampal cells respond to nanomolar concentrations of muscimol. *Dev. Brain Res.* 0, 1–8.
- Fox, K. (1995). The critical period for long-term potentiation in primary sensory cortex. *Neuron* 15, 485–488.
- Fox, K., Sato, H., and Daw, N. (1989). The location and function of NMDA receptors in cat and kitten visual cortex. *J. Neurosci.* 9, 2443–2454.
- Fukuda, A., Mody, I., and Prince, D.A. (1993). Differential ontogenesis of presynaptic and postsynaptic GABA_B inhibition in the rat somatosensory cortex. *J. Neurophysiol.* 70, 448–452.
- Gaiarsa, J.L., Corradetti, R., Cherubini, E., and Ben-Ari, Y. (1990). Modulation of GABA-mediated synaptic potentials by glutamatergic agonists in neonatal CA3 rat hippocampal neurons. *Eur. J. Neurosci.* 3, 301–309.
- Gaiarsa, J.L., McLean, H., Congar, P., Leinekugel, X., Khazipov, R., Tsseeb, V., and Ben-Ari, Y. (1995). Postnatal maturation of Gamma-Aminobutyric acid A and B-mediated inhibition in the CA3 hippocampal region of the rat. *J. Neurobiol.* 26, 339–349.
- Goodman, C.S., and Shatz, C.J. (1993). Developmental mechanisms that generate precise patterns of neuronal connectivity. *Cell/Neuron* 72/10 (suppl.), 77–98.
- Gu, X., and Spitzer, N.C. (1995). Distinct aspects of neuronal differentiation encoded by frequency of spontaneous Ca^{2+} transients. *Nature* 375, 784–787.
- Hales, T.G., Sanderson, M.J., and Charles, A.C. (1994). GABA has excitatory actions on GnRH-secreting immortalized hypothalamic (GT1-7) neurons. *Neuroendocrinology* 59, 297–308.
- Hanse, E., Garaschuk, O., and Konnerth, A. (1996). Early network oscillations in the developing hippocampus. *Soc. Neurosci.*, 26, 774.6.
- Hara, M., Inoue, M., Yasukura, T., Ohnishi, S., Mikami, Y., and Inagaki, C. (1992). Uneven distribution of intracellular Cl^- in rat hippocampal neurons. *Neurosci. Lett.* 143, 135–138.
- Hestrin, S. (1992). Developmental regulation of NMDA receptor-mediated synaptic currents at a central synapse. *Nature* 357, 686–689.
- Kaila, K., and Voipio, J. (1994). Ionic basis of GABA_A receptor channel function in the nervous system. *Prog. Neurobiol.* 42, 489–537.
- Kandler, K., and Katz, L.C. (1995). Neuronal coupling and uncoupling in the developing nervous system. *Curr. Opin. Neurobiol.* 5, 98–105.
- Kanter, E.D., and Haberly, L.D. (1993). Associative long-term potentiation in piriform cortex slices requires GABA_A blockade. *J. Neurosci.* 13, 2477–2482.
- Kanter, E.D., Kapur, A., and Haberly, L.B. (1996). A dendritic GABA_A -mediated IPSP regulates facilitation of NMDA-mediated responses to burst stimulation of afferent fibers in piriform cortex. *J. Neurosci.* 16, 307–312.
- Kao, J.P.Y., Harootunian, A.T., and Tsien, R.Y. (1989). Photochemically generated cytosolic calcium pulses and their detection by Fluo-3. *J. Biol. Chem.* 264, 8179–8184.
- Katz, L.C. (1993). Coordinate activity in retinal and cortical development. *Curr. Opin. Neurobiol.* 3, 93–99.
- Khalilov, I., Khazipov, R., Leinekugel, X., Feger, J., and Ben-Ari,

- Y. (1996). Intracellular blockade of GABA_A receptors as a tool to investigate neuronal network activity. *Soc. Neurosci.* 26 221.1.
- Khazipov, R., Ragozin, D., and Bregestovski, P. (1995). Kinetics and Mg²⁺ block of N-Methyl-D-Aspartate receptor channels during postnatal development of hippocampal CA3 pyramidal neurons. *Neuroscience* 69, 1057–1065.
- Khazipov, R., Leinekugel, X., Khalilov, I., Gaïarsa, J.L., and Ben-Ari, Y. (1997). Synchronization of GABAergic interneuronal network in CA₃ subfield of neonatal rat hippocampal slices. *J. Physiol. (Lond.)*, in press.
- Kirkwood, A., Lee, H., and Bear, M.F. (1995). Co-regulation of long-term potentiation and experience-dependent synaptic plasticity in visual cortex by age and experience. *Nature* 375, 328–331.
- Komatsu, Y., and Iwakiri, M. (1993). Long-term modification of inhibitory synaptic transmission in developing visual cortex. *Neuroreport* 4, 907–910.
- Lauder, J.M. (1993). Neurotransmitters as growth regulatory signals: role of receptors and second messengers. *Trends Neurosci.* 16, 233–240.
- Leinekugel, X., Tseeb, V., Ben-Ari, Y., and Bregestovski, P. (1995). Synaptic GABA_A activation induces Ca⁺⁺ rise in pyramidal cells and interneurons from rat neonatal hippocampal slices. *J. Physiol. (Lond.)* 487, 319–329.
- Lipton, S.A., and Kater, S.B. (1989). Neurotransmitter regulation of neuronal outgrowth, plasticity and survival. *Trends Neurosci.* 12, 265–270.
- LoTurco, J.J., Blanton, M.G., and Kriegstein, A.R. (1991). Initial expression and endogenous activation of NMDA channels in early neocortical development. *J. Neurosci.* 11, 792–799.
- LoTurco, J.J., Owens, D.F., Heath, M.J.S., Davis, M.B.E., and Kriegstein, A.R. (1995). GABA and glutamate depolarize cortical progenitor cells and inhibit DNA synthesis. *Neuron* 15, 1287–1298.
- Luhmann, H.J., and Prince, D.A. (1991). Postnatal maturation of the GABAergic system in rat neocortex. *J. Neurophysiol.* 65, 247–263.
- Malenka, R.C., and Nicoll, R.A. (1993). NMDA-receptor-dependent synaptic plasticity: multiple forms and mechanisms. *Trends Neurosci.* 16, 521–527.
- Marty, S., Berninger, B., Carroll, P., and Thoenen, H. (1996). GABAergic stimulation regulates the phenotype of hippocampal interneurons through the regulation of Brain-Derived Neurotrophic Factor. *Neuron* 16, 565–570.
- Mayer, M.L., Westbrook, G.L., and Guthrie, P.B. (1984). Voltage-dependent block by Mg⁺⁺ of NMDA responses in spinal cord neurons. *Nature* 309, 261–263.
- McBain, C., and Dingledine, R. (1992). Dual-component miniature excitatory synaptic currents in rat hippocampal CA3 pyramidal neurons. *J. Neurophysiol.* 68, 16–27.
- McLean, H.A., Rovira, C., Ben-Ari, Y., and Gaïarsa, J.L. (1995). NMDA-dependent GABA-A-mediated polysynaptic potentials in the neonatal rat hippocampal CA3 region. *Eur. J. Neurosci.* 7, 1442–1448.
- McLean, H.A., Caillard, O., Ben-Ari Y., and Gaïarsa, J.L. (1996). Bidirectional plasticity expressed by GABAergic synapses in the neonatal rat hippocampus. *J. Physiol. (Lond.)* 496, 471–477.
- Medina, I., Filippova, N., Barbin, G., Ben-Ari, Y., and Bregestovski, P. (1994). Intracellular Ca²⁺ inactivates NMDA currents. *J. Neurophysiol.* 72, 456–465.
- Miyakawa, H., Ross, W.N., Jaffe, D., Callaway, J.C., Lasser-Ross, N., Lisman, J.E., and Johnston, D. (1992). Synaptically activated increases in Ca⁺⁺ concentration in hippocampal CA1 pyramidal cells are primarily due to voltage-gated Ca⁺⁺ channels. *Neuron* 9, 1163–1173.
- Monyer, H., Burnashev, N., Laurie, D., Sakmann, B., and Seuberg, P.H. (1994). Developmental and regional expression in the rat brain and functional properties of four NMDA receptors. *Neuron* 12, 529–540.
- Müller, W., and Connor, J.A. (1991). Dendritic spines as individual neuronal compartments for synaptic Ca⁺⁺ responses. *Nature* 354, 73–76.
- Nowak, L., Bregestovski, P., Ascher, P., Herbert, A., and Prochiantz, A. (1984). Magnesium gates glutamate-activated channels in mouse central neurons. *Nature* 307, 462–465.
- O'Donovan, M.J., Sernagor, E., Sholomenko, G., Ho, S., Antal, M., and Yee, W. (1992). Development of spinal motor networks in the chick embryo. *J. Exp. Zool.* 261, 261–273.
- Obrietan, K., and van den Pol, A.N. (1995). GABA neurotransmission in the hypothalamus: developmental reversal from Ca⁺⁺ elevating to depressing. *J. Neurosci.* 15, 5065–5077.
- Pollard, H., Khrestchatsky M., Moreau J., and Ben-Ari Y. (1993). Transient expression of the NR2C subunit of the NMDA receptor in developing rat brain. *Neuroreport* 4, 411–414.
- Rakic, P., and Komuro, H. (1995). The role of receptor-channel activity in neuronal cell migration. *J. Neurobiol.* 26, 299–315.
- Redburn, D., and Schousboe, A. (1987). Neurotrophic activity of GABA during development. *Neurol. Neurobiol.* 32, 1–227.
- Regher, W.G., and Tank, D.W. (1992). Calcium concentration dynamics produced by synaptic activation of CA1 hippocampal pyramidal cells. *J. Neurosci.* 12, 4202–4223.
- Reichling, D.B., Kyrozin, A., Wang, J., and MacDermott, A.B. (1994). Mechanisms of GABA and glycine depolarization-induced calcium transients in rat dorsal horn neurons. *J. Physiol. (Lond.)* 476, 411–421.
- Represa, A., Tremblay, E., and Ben-Ari, Y. (1989). Transient increase of NMDA-binding sites in human hippocampus during development. *Neurosci. Lett.* 99, 61–66.
- Rohrbough, J., and Spitzer, N.C. (1996). Regulation of intracellular Cl⁻ levels by Na⁺-dependent Cl⁻ cotransport distinguishes depolarizing from hyperpolarizing GABA_A receptor-mediated responses in spinal neurons. *J. Neurosci.* 16, 82–91.
- Rusanescu, G., Qi, H., Thomas, S.M., Brugge, J.S., and Halegoua, S. (1995). Calcium influx induces neurite growth through a Src-Ras signaling cassette. *Neuron* 15, 1415–1425.
- Scherer, W.S., and Udin, S.B. (1989). N-methyl-D-aspartate antagonists prevent interaction of binocular maps in Xenopus tectum. *J. Neurosci.* 9, 3837–3843.
- Serafini, R., Valeev, A.Y., Barker, J.L., and Poulter, M.O. (1995). Depolarizing GABA-activated Cl⁻ channels in embryonic rat spinal and olfactory bulb cells. *J. Physiol. (Lond.)* 488, 371–386.
- Sivilotti, L., and Nistri, A. (1991). GABA receptor mechanism in the central nervous system. *Prog. Neurobiol.* 36, 35–92.
- Spoerri, P.E. (1988). Neurotrophic effects of GABA in cultures of embryonic chick brain and retina. *Synapse* 2, 11–22.
- Staley, K.J., and Mody, I. (1992). Shunting of excitatory input to dentate gyrus granule cells by a depolarizing GABA_A receptor-mediated postsynaptic conductance. *J. Neurophysiol.* 68, 197–212.
- Staley, K.J., Soldo, B.L., and Proctor, W.R. (1995). Ionic mechanisms of neuronal excitation by inhibitory GABA_A receptors. *Science* 269, 977–981.
- Strecker, G.J., Jackson, M.B., and Dudek, F.E. (1994). Blockade of NMDA-activated channels by magnesium in the immature rat hippocampus. *J. Neurophysiol.* 72, 1538–1548.
- Tremblay, E., Roisin, M.-P., Represa, A., Charriaut-Marlangue, C., and Ben-Ari, Y. (1988). Transient increased density of NMDA binding sites in the developing rat hippocampus. *Brain Res.* 467, 393–396.
- Tsumoto, T., Hagiwara, K., Sato, H., and Hata, Y. (1987). NMDA receptors in the visual cortex of young kittens are more effective than those of adult cats. *Nature* 327, 513–514.
- Wang, J., Reichling, D.B., Kyrozin, A., and MacDermott, A.B. (1994). Developmental loss of GABA- and glycine-induced depolarization and Ca⁺⁺ transients in embryonic rat dorsal horn neurons in culture. *Eur. J. Neurosci.* 6, 1275–1280.
- Wigstrom, H., and Gustafsson, B. (1983). Facilitated induction of hippocampal long-lasting potentiation during blockade of inhibition. *Nature* 270, 356–357.
- Wong, R.O.L., Meister, M., and Shatz, C.J. (1993). Transient period

of correlated bursting activity during development of the mammalian retina. *Neuron* **11**, 923–938.

Wu, W.L., Ziskind-Conhaim, L., and Sweet, M.A. (1992). Early development of glycine- and GABA-mediated synapses in rat spinal cord. *J. Neurosci.* **12**, 3935–3945.

Yuste, R., and Katz, L.C. (1991). Control of postsynaptic Ca^{++} influx in developing neocortex by excitatory and inhibitory neurotransmitters. *Neuron* **6**, 333–344.

Yuste, R., Nelson, D.A., Rubin, W.W., and Katz, L.C. (1995). Neuronal domains in developing neocortex: mechanisms of coactivation. *Neuron* **14**, 7–17.

Zhang, L., Spigelman, I., and Carlen, P.L. (1991). Development of GABA-mediated, chloride-dependent inhibition in CA1 pyramidal neurones of immature rat hippocampal slices. *J. Physiol. (Lond.)* **444**, 25–49.